AD-A127 565 THE VARIATION OF FINESTRUCTURE ACROSS A MESOSCALE FEATURE(U) NAVAL RESEARCH LAB WASHINGTON DC R P MIED ET AL. 11 MAY 83 NRL-MR-5062 1/1

UNCLASSIFIED F/G 8/3 NL

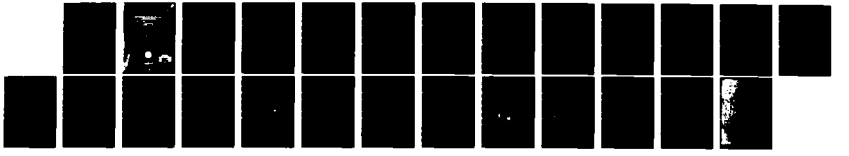

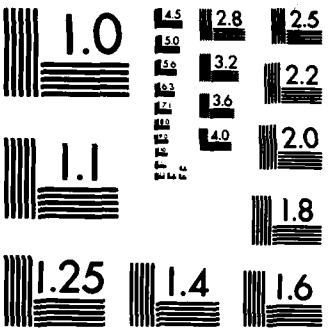

SECURITY CLASSIFICATION OF THIS PAGE (When Data Entered)

REPORT DOCUMENTATION PAGE	READ INSTRUCTIONS BEFORE COMPLETING FORM
1. REPORT NUMBER: NRL Memorandum Report 5062 — 2. GOVT ACCESSION NO.: AD-A127565	3. RECIPIENT'S CATALOG NUMBER:
4. TITLE (and Subtitle): THE VARIATION OF FINESTRUCTURE ACROSS A MESOSCALE FEATURE	5. TYPE OF REPORT & PERIOD COVERED: Interim report on a continuing NRL problem.
	6. PERFORMING ORG. REPORT NUMBER:
7. AUTHOR(s): R. P. Mied, L. J. Morris, A. F. Schuetz, and G. J. Lindemann	8. CONTRACT OR GRANT NUMBER(s):
9. PERFORMING ORGANIZATION NAME AND ADDRESS: Naval Research Laboratory, Washington, D. C. 20375	10. PROGRAM ELEMENT, PROJECT, TASK AREA & WORK UNIT NUMBERS: 63704; R1299-OS; 43-1148-0-2
11. CONTROLLING OFFICE NAME AND ADDRESS: Naval Oceanographic Research and Development Activity, NSTL Station, MS 39529	12. REPORT DATE: May 11, 1983
	13. NUMBER OF PAGES: 23
14. MONITORING AGENCY NAME & ADDRESS(if different from Controlling Office)	15. SECURITY CLASS. (of this report): UNCLASSIFIED
	15a. DECLASSIFICATION/DOWNGRADING SCHEDULE:

16. DISTRIBUTION STATEMENT (of this Report)

Approved for public release; distribution unlimited.

17. DISTRIBUTION STATEMENT (of the abstract entered in Block 20, if different from Report)

18. SUPPLEMENTARY NOTES

19. KEY WORDS (Continue on reverse side if necessary and identify by block number)

Finestructure
Dropped spectra
Current shear
Mesoscale currents
Gulf Stream ring

20. ABSTRACT (Continue on reverse side if necessary and identify by block number)

The 602 XBT drops from the June 1979 LYNCH cruise are examined for the finestructure variation across the FREDDEX eddy. All of the spectra are scaled with the Brunt-Vaisala frequency and are observed to collapse to a single form inside and outside the ring. A correlation is observed between the variance of the scaled finestructure spectrum and the horizontal and vertical mesoscale current shears, which can attain maxima of orders $10^{-6}S^{-1}$ and $(10^{-3}S^{-1}$ respectively in some parts of the ring.

DD FORM 1 JAN 73 1473 EDITION OF 1 NOV 65 IS OBSOLETE
S/N 0102-014-6601

SECURITY CLASSIFICATION OF THIS PAGE (When Data Entered)

1/1000 S

1/1000000 S

CONTENTS

THE VARIATION OF FINESTRUCTURE ACROSS A MESOSCALE FEATURE

I. Background

The performance of nonacoustic and acoustic submarine detection systems is crucially dependent upon the finestructure in the ocean, and it is for these reasons that we are interested in the level of the finestructure variance density and the variation of this spectrum across mesoscale features.

Because of the theoretical intractability of calculating an internal wave equilibrium spectrum from first principles, oceanographers have been greatly aided by the series of papers by Garrett and/or Munk (1972, 1975, 1981) in which the original empirical spectrum (GM72) is specified and two iterative improvements (GM75, GM79) have been proposed to take additional data into account. It is this general form with which all internal wave measurements are presently gauged, and we continue that practice in this work. In particular, we shall be interested in how well the scaled, dropped displacement spectra conform to the analytical representation of the GM79 model, and in turn, how this form varies across the mesoscale.

Of principal concern here is the correlation of strong horizontal and vertical shears with the energy level of the Garrett and Munk spectral model. We suspect that the level of coupling between shear and the dropped spectrum may be much stronger than expected from simple kinematic considerations of current variations. In a related problem, for example, mesoscale variations in the level of temperature finestructure have been

Manuscript approved February 8, 1983.

observed by Belyayev and Nozdrin (1979) in the vicinity of a front, while Gargett (1978) and Williams (1981) have observed intrusive features in the vicinity of a front. It is, therefore, crucial that we understand fine structure variability over mesoscale features, and it is the goal toward which this work is directed.

II. Introduction

During the period 3 June - 25 June 1979, the USNS LYNCH transitted across the Gulf Stream to an area northwest of Bermuda to survey a Gulf Stream ring (Mied, Lindemann, and Schuetz, 1981). During that time interval, over six hundred XBT's were dropped. These reveal that the eddy is oval shaped, and that this second mode azimuthal wave propagates cyclonically while regularly exchanging energy with the mean eddy flow (Mied, Lindemann, and Bergin, 1983).

In an earlier report (Mied, Lindemann, and Schuetz, 1981), we espoused the view that the main independent variables in determining the level of finestructure within a mesoscale feature are the vertical and horizontal shears. With this in mind, the first report sought to establish what we felt was an appropriate base knowledge for future work. The current structure was inferred from the thermal wind equation using data from XBT drops and STD casts taken by NAVOCEANO (Blumenthal, private communication, 1981).

In this report, we address the second phase of the work, in which the XBT's are now used to determine the dropped temperature spectra of that finestructure. The reporting of the differences in the level of these spectra as a function of their position within the eddy is the purpose of this report.

Finestructure is a term which we use to designate the spatial fluctuation of thermodynamic or kinematic variables of scales > 1 m. The source of this variation - whether reversible or irreversable - is not considered. The significant point is that the 1-50 m vertical wavelength range is of interest to us and this is the range for which the XBT is suited. We would

like to take advantage of finestructure measurements in the presence of a strong shear but not incur the penalty of intrusive finestructure encountered near fronts.

One type of intense shear field with no appreciable difference in T-S properties is the deeper portion of a cold-core Gulf Stream ring. In this class of flow, shelf water is surrounded by Sargasso sea water but, as noted above, their T-S curves for temperatures below 17°C are effectively identical and do not display the type of differences which are present, for example, across the sub-Arctic front. Thus we have an advantage of being able to measure finestructure in a strongly sheared environment without having to accept the complication of potentially strong sources of finestructure from intrusive instabilities.

Our interest in dropped finestructure spectra in strong currents and shears is two-fold. First, both Frankignoul (1976) and Ruddick and Joyce (1979) have found that shear/internal wave coupling is much weaker than predicted by Müller (1976) for currents $\lesssim$ 25 cm/sec and concomitantly small shears. In contrast with this, the currents and shears found in rings are certainly among the largest in the oceans, so that if any effect is to be found, it will most likely appear here. Second, these authors concentrated upon spectra from current meters and examined internal waves with horizontal wavelengths of $\lesssim$ 1 km. By examining dropped spectra of thermodynamic variables, we focus upon a class of physics heretofore ignored. On the other hand the coupling between long waves and mesoscale shear is not examined, because we are concentrating here upon the signature of the coupling between shears and much smaller scale waves, mixing events, and turbulence.

III. The Internal Wave Spectrum

The first fairly realistic, workable internal wave spectrum was actually the GM75 model,; however several disadvantages of this formulation soon became apparent. Cairns and Williams (1976) found that the vertical wavenumber (k) dependence of the spectrum is proportional to k^{-2} instead of $k^{-5/2}$ as in GM75. Using this information, Desaubies (1976) produced an analytical formulation which obviated the rigorous, but inconvenient, formulation in terms of normal modes. In this revised spectrum, he eliminated the requisite exponential stratification of the GM72 model and produced a spectral form with only the energy level and bandwidth as parameters. Some of these changes were in turn incorporated into the GM79 version, but we shall refer to the work of Desaubies because of the ease with which it may be used.

The dropped displacement spectrum is

$$DS\zeta\ (k) = \int_f^n \overline{Z}^2\ E(k,\omega)\ dw \qquad \text{(III.1)}$$

where $\overline{Z}^2 = b^2N(\omega^2-f^2)n^{-1}\omega^{-2}$, $E(k,\omega) = \frac{2E}{\pi}\ k_*^{-1}\ A(k/k_*)f\omega^{-1}\ (\omega^2-f^2)^{-1/2}$

$$k_* = t(n^2-\omega^2)^{1/2},\quad r = Eb^2N,\quad A(k/k_*) = 2\pi^{-1}\ [1+(k/k_*)^2]^{-1},$$

$$t = j/2bn.$$

Here f = 2 · (earth's rotation time) · sin (latitude), while N and n are the reference and <u>in situ</u> Brunt-Vaisala frequencies respectively.

The spectrum (III.1) may be written in the more compact form

$$DS\zeta\ (k) = \left(\frac{2}{\pi}\right)^2 \frac{rt}{k^2+k_*^2}\ \frac{f}{n}\int_f^n \frac{(\omega^2-f^2)^{1/2}\ (n^2-\omega^2)^{1/2}}{\omega^3}\ d\omega \qquad \text{(III.2)}$$

Although $k_* = k_*(\omega)$, we have taken advantage of the fact that

$$k_* = t(n^2-\omega^2)^{1/2} \simeq tn = \frac{jn}{2bN} \sim \frac{6}{2\cdot 1.3\text{-}10^3\ m} \sim 7\ .\ 10^{-4}\ \text{cpm} \ll k\ .$$

H^2O

Carrying k_* through the ω-integral therefore does not materially alter the value of the integral; retained in this form, it assumes its alternate role as a bandwidth.

We may define

$$I \equiv \frac{f}{n} \int_f^n \frac{(\omega^2-f^2)^{1/2}\,(n^2-\omega^2)^{1/2}}{\omega^3}\,d\omega. \qquad \text{(III.3)}$$

If we introduce $\Omega = \omega/f$ and recall that in the ocean, $n/f >> 1$, we see that

$$I \simeq \int_1^\infty \frac{(\Omega^2-1)^{1/2}}{\Omega^3}\,d\Omega .$$

An integration by parts yields

$$I = 1/2 \int_1^\infty \frac{d\Omega}{\Omega(\Omega^2-1)^{1/2}} ,$$

which may be evaluated with the substitution $\Omega = \cosh t$:

$$I \simeq 1/2 \int_0^\infty \operatorname{sech} t\, dt = \pi/4. \qquad \text{(III.4)}$$

Eq. (III.2-4) may be combined to yield the dropped displacement spectrum

$$DS_\zeta(k) = \frac{rt}{\pi(k^2+k_*^2)} , \qquad \text{(III.5)}$$

which may in turn be integrated over all k to yield the variance of the displacement

$$\langle\zeta^2\rangle = \frac{rt}{\pi} \int_0^\infty \frac{dk}{k^2+k_*^2} .$$

with the variable change $k/k_* = \tan z$, one may easily calculate

$$\langle\zeta^2\rangle = \frac{rt}{2k_*}, \qquad \text{(III.6)}$$

so that (III.5) becomes

$$DS_\zeta(k) = \frac{2\langle\zeta^2\rangle k_*}{\pi(k^2+k_*^2)} \quad , \qquad \text{(III.7)}$$

It is an important part of this formulation that $rt = (Eb^2N)(j/2bN) = \frac{jbE}{2}$ (m^2). Thus, the spectrum is completely specified when its energy level and bandwidth are known.

IV. Treatment of Data

As noted in Section II, the data set consists of 602 temperature traces obtained by using T-5 and T-7 types of XBTs. A careful, multistep editing procedure (Mied, Lindemann and Schuetz, 1981) has reduced this set to 515 high quality drops. Because the mean temperature varies greatly with depth, and because we are interested in the 1-50 m wavelength range of the vertical spectrum, we have examined depth segments of approximately 100 m selected from different depths of the cast. These data windows are located at 400 ± 50 m, 700 ± 50 m, 1000 ± 50 m, and 1200 ± 50 m. Naturally, the T-7 probes cannot provide these latter two sets because of their relatively shallow survey capability (~ 850 m).

The temperature data were detrended by fitting a linear curve to the numbers using a least squares routine. The difference between this fitted (mean) temperature as a function of depth and the original data was fourier transformed. The resulting temperature spectrum $DS_T(k)$ was then converted into a dropped isotherm displacement spectrum $DS_\zeta(k)$ by scaling with the local temperature gradient obtained from the polynomial fit (and thus assumed constant over the 100 m depth range):

$$DS_\zeta(k) = \frac{DS_T(k)}{(dT/dz)^2}$$

These "100 m depth" segments do not measure precisely 100 m, however. Because the rate of fall of an XBT decreases slowly as wire is unwound, the constant-sampling-rate digital temperature record becomes slightly more dense with depth. A T-5 XBT falls according to the formula (Mied, Lindemann, and Bergin, 1981)

$$z = 6.64t - .00177t^2 \ .$$

With a sampling rate 30 Hz, we calculate the data intervals at 400 m and 1200 m depths to be .214 m and .199 m respectively. Since the "100 m" depth segments are comprised of 512 data points (511 intervals), the data records at 400, 700, 1000 and 1200 m actually vary between 109.4 and 101.7m in length.

V. Dropped Spectra of Isotherm Displacement

Embedded within the spectrum (III.5) is a scaling which adjusts the spectral level and the vertical wavenumber with the Brunt-Vaisala frequency of the medium. To see this, we note that $k_* \simeq tn = \frac{jn}{2bN}$. Then III.5 may be seen to indicate that

$$DS_\zeta(k) = \frac{rt}{\pi k_*^2 (k^2/k_*^2+1)} \simeq \frac{r}{\pi (tn)^2 [(k/tn)^2+1]}.$$

or $n^2 DS_\zeta(k) \propto (k/n)^{-2}$ for $k >> k_*$.

In Figure 1 we plot $\left(\frac{n}{1 \text{ cph}}\right)^2 DS_\zeta$ in $(m^2 \text{ cpm}^{-1})$ as a function of

$\frac{1 \text{ cph}}{n}$ k (in cpm) for XBT #53. This scaling works to collapse the spectra for a typical open-ocean XBT drop, away from an mesoscale features.

That all four spectra collapse fairly well and roll off more or less as $(k/k_*)^{-2}$ is in support of the scaling in the GM79 model. It is all the more remarkable in view of the variation of the Brunt-Vaisala frequency distribution n(Z) with depth (Figure 2), which exhibits a range in n spanning a factor of 5.

One disadvantage of scaling the wavenumber with n(Z) is that the actual in situ wavenumbers k are not readily retrieved from graphs such as Figure 1. Now that we have demonstrated the efficacy of the GM79 spectral scaling for the data, we will find it useful to abandon this rigorous mode of scaling. Of more direct physical relevance is the empirical fact that spectra scale as n^{-1} when plotted as a function of k. We shall therefore display $\left(\frac{n}{1\ cph}\right)$ DSF $_\zeta$ (k) as a function of k in all other plots appearing in this report.

VI. Mesoscale Variation of the GM79 Spectrum

The underlying idea in this work is to show that although the properly scaled background spectrum variance fluctuates a bit, the presence of velocity shear is correlated with a discernable change in the spectral level. But, precisely what is the variation of the overall level of the background spectrum in the open ocean? A convenient and succinct way to express this fluctuation is to examine the variance of the dropped displacement spectrum ($\langle\zeta^2\rangle$). The limited length of the data records (~ 100 m) indicates that the variance cannot be defined for $0<k<\infty$. Instead we are limited on the low-k side by the record length and on the high-k end by the sampling rate (30 Hz). As the XBT falls at a speed ~ 6 ms^{-1}, we expect that the spectral values in wavelengths shorter than

$2 \cdot 6\ ms^{-1}/30s^{-1} = 0.4$ m will be meaningless; the Nyquist wavenumber is thus k = 2.5 cpm. However, examination of the data indicates that in order to avoid contamination of the spectral values by the noise floor, we should only consider data for $k \leq 0.4$ cpm ($\lambda \geq 2.5$ m). Considering these limitations on the data, we define our variance to be the integral of the spectral energy density over the wavenumber decade .04 cpm $\leq k \leq$ 0.4 cpm ($2.5 \leq \lambda \leq 25$ m). Although the record is only approximately 100 m long, the variance wavenumber interval is precise, because the spectrum is interpolated. In Figure 3, we note $n\langle\zeta^2\rangle$ along the ship track in the upper ocean between the Gulf Stream and the eddy. The depths sampled are the same as those examined previously, and we see that the scaled variance of the displacement spectrum is horizontally quite variable. At some points along the tracks, we can discern trends in the variance, while at other positions, its fluctuation seems random. Some associated spectra positioned along the ship track are shown in Figure 4. There are certainly no clues in these graphs as to the origin of the observed variance fluctuation. That is, no one portion of the spectrum appears enhanced over another. Moreover, all of these scaled spectra collapse as expected. Nevertheless, the amount of variation seems surprising, because these XBT drops are well away from any notable current system. One might think that the very large variances are the result of instrument failure or a computational mistake. This is not the case. Each XBT trace with an unusually large variance has been carefully examined, along with those around it, and accepted as being real. For example, the large scaled variance present at 67.35°W (in the 650-750 m range) came from XBT #60 and showed a large

temperature anomaly at about the same depth as did XBT #59, which is 7.33 km removed. A knowledge of this ambient, natural fluctuation in the level of the variance will prove useful below in differentiating between natural background variations and significant variance alteration in regions of large shear.

If a correlation between finestructure variance and current shear exists, then it should be apparent as different XBT's along the ship track within the eddy are examined. In particular, geostrophy dictates that vertical current shear and isopycnal slopes are linearly related. When the slope of an isothermal surface is the largest, the vertical shear should be a maximum. In addition, the horizontal shear has two radial positions at which it assumes maxima. These larger shears should, in turn, be located where atypically different spectral levels (hence variances) are found. The postulated finestructure/mesoscale shear correlation should thus be characterized by anomalous variances where the horizontal or vertical current shear is large.

In order to test the strength of this correlation, we have regressed the scaled displacement variances (n/1 cpm) $< T'^2 > / (d\bar{T}/dz)^2$ onto the vertical mesoscale current shear $[(dU/dz)^2 + (dV/dz)^2]^{1/2}$ for all four depths of both eddy snapshots (Figure 5). This calculation clearly shows that as the shear is increased, the scaled variance is likely to decrease. This is not a strong trend, but it can be discerned visually, and is given strong credence because of the large number (463) of observations used to derive the regression coefficient of -.426.

One would also think, however, that there might be a correlation between the variance and the horizontal shear $[(dU/dy)^2 + (dV/dx)^2]^{1/2}$.

To test this hypothesis, we have regressed the variance onto the horizontal shear (Figure 6), and we see that the correlation is also negative, but somewhat weaker (-.293). Since the maximum horizontal and vertical shears are $O(10^{-6}s^{-1})$ and $O(10^{-3}s^{-1})$ respectively, the apparent closeness of their correlations with the variance (-.293 and -.426) is interesting. We interpret this result as follows. The primary correlation is between the variance and the vertical shear. The physical coherence of the ring, however, dictates that the regression of the vertical shear upon the horizontal shear be high (0.667, in fact). We believe that the -.293 for the variance/horizontal shear regression simply reflects the correlation between the vertical and horizontal shears, and does not reflect a causal relationship.

VII. Conclusions

The overall goal of the research reported in this series of reports is to qualitatively correlate the level of the finestructure with the horizontal and vertical mesoscale shear which is present. This research is needed to establish the general level of fluctuation of the ambient finestructure level over mesoscale features.

We have taken a step-by-step approach to the problem by first calculating the levels of the shears within the eddy (Mied, Lindemann, and Schuetz, 1981). The next step has been to examine the finestructure and note how it varies over the "quiescent" mesoscale and in regions of shear.

In this paper then, we have endeavored to show that the scaled, dropped spectrum of the isotherm displacement is quite variable over the mesoscale. Using the temperature data from T-5 and T-7 XBT's dropped in the quiescent ocean and within a Gulf Stream ring, we have established the following facts.

1. The dropped spectra at different depths all collapse in the absence of current shear, provided they are scaled with n/1 cph.

2. Within the eddy, scaled spectra from regions of high vertical shear are likely to have lower energy level than those from the non-sheared (central and outer) portions of the eddy.

3. The scaled displacement variance decreases moderately ($R = -.426$) with increasing vertical shear, but only weakly with increasing horizontal shear ($R = -.293$). This latter figure is specious because it is probably due to the high correlation between horizontal and vertical shear.

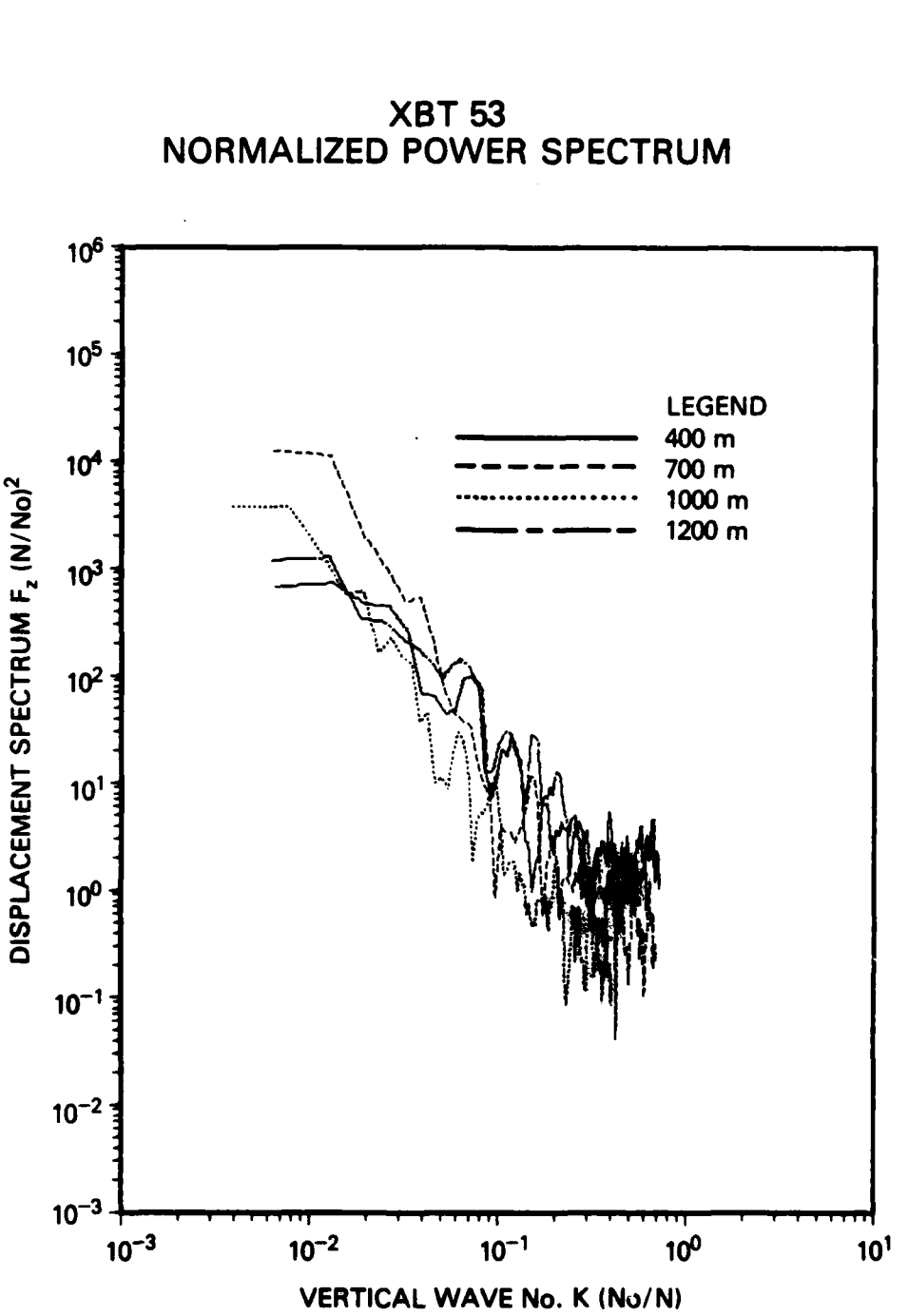

Fig. 1 — The scaled dropped displacement spectrum (n/1 cph)^2 F_ζ (k) of XBT #53 as a function of the scaled wavenumber k (1 cph/n). The location is 35.3045°N, 67.9212°W and is away from any ring currents and the Gulf Stream. The depths are 400, 700, 1000, and 1200 m. The parameter S=3 indicates that for all but the spectral value at the lowest wavenumber, the spectrum displayed is actually the band average of the original spectral estimate and the ones to either side in wavenumber space.

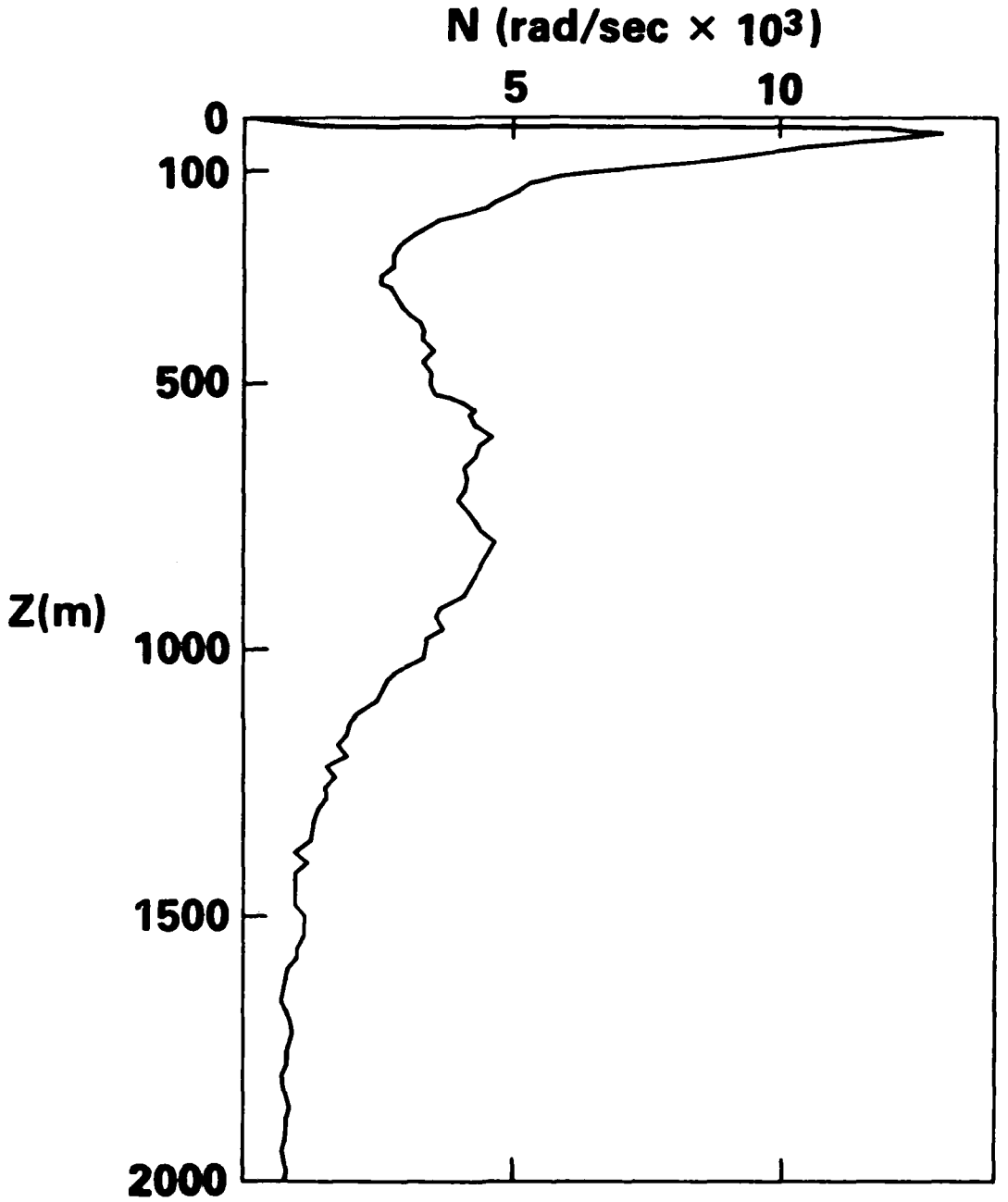

Fig. 2 — An average of an ensemble of Brunt-Vaisala frequency distributions for all of the XBT's shown in Fig. 3 in the region outside of the eddy and away from the Gulf Stream.

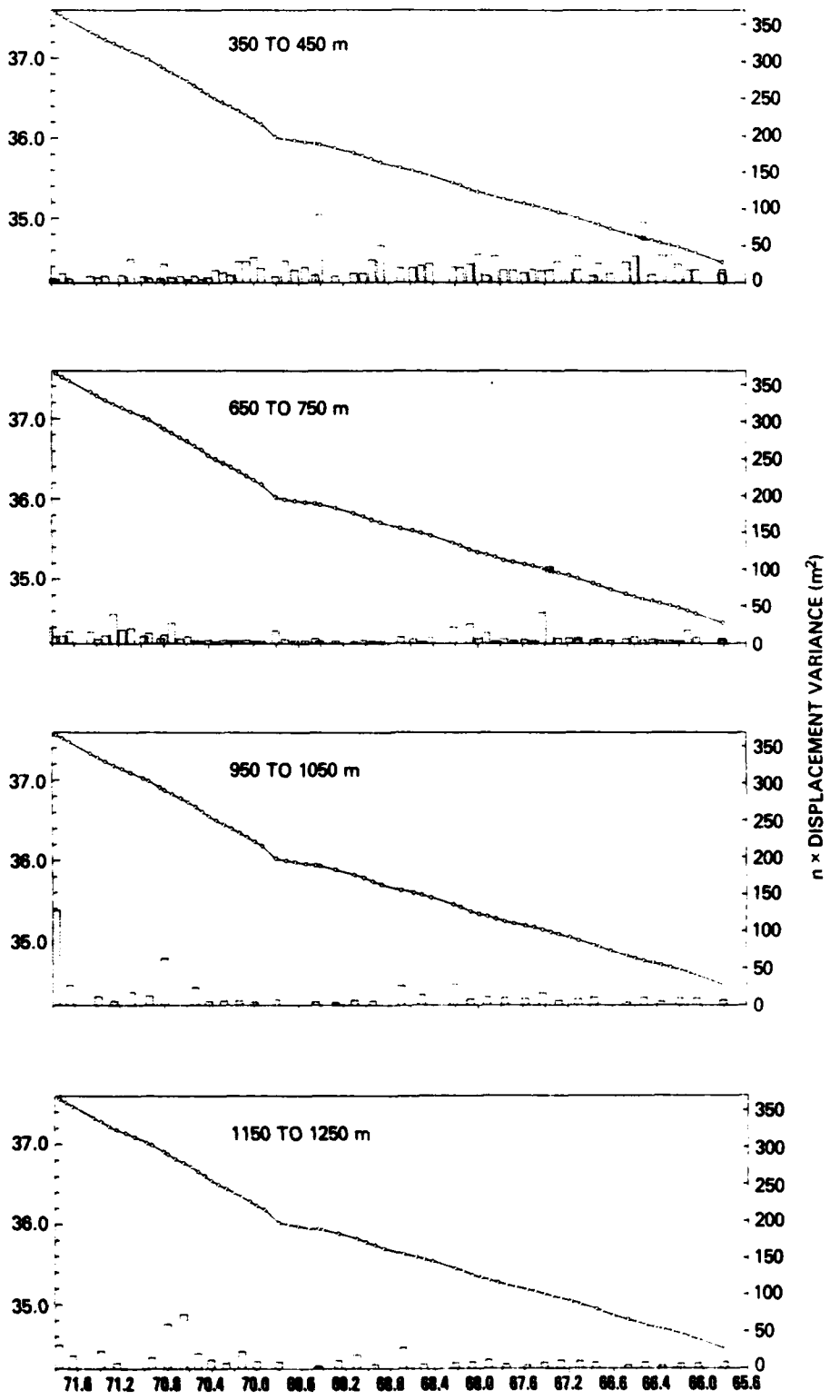

Fig. 3 — The scaled displacement variance (n/1 cph) $<\zeta^2>$ at the four standard depths along the open-ocean track between the Gulf Stream and the eddy.

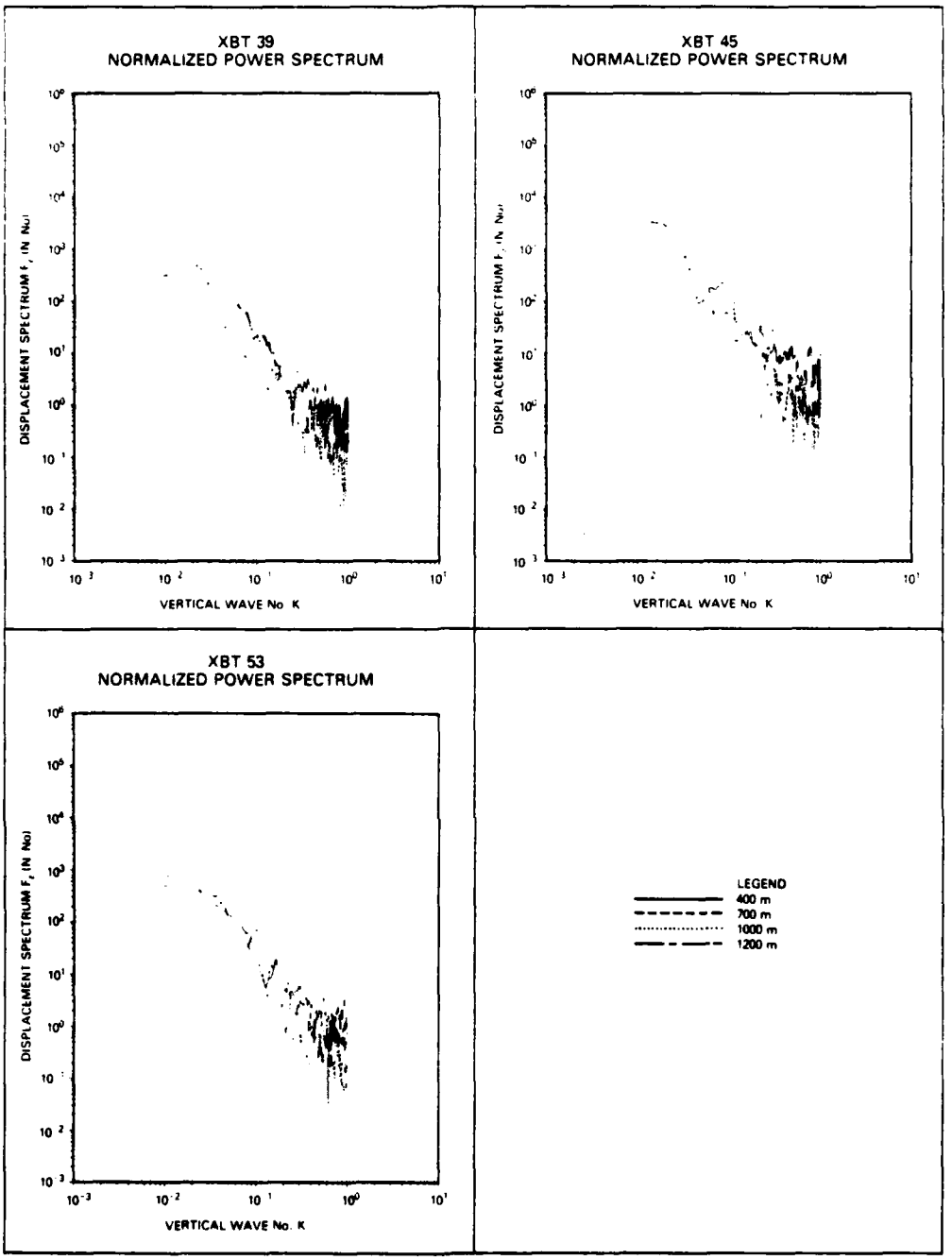

Fig. 4 — Three examples of the scaled displacement spectra (n/1 cph) F_ζ (k) as a function of k (cpm) for the depths 400, 700, 1000, and 1200 m at selected points along the ship track in the open ocean.

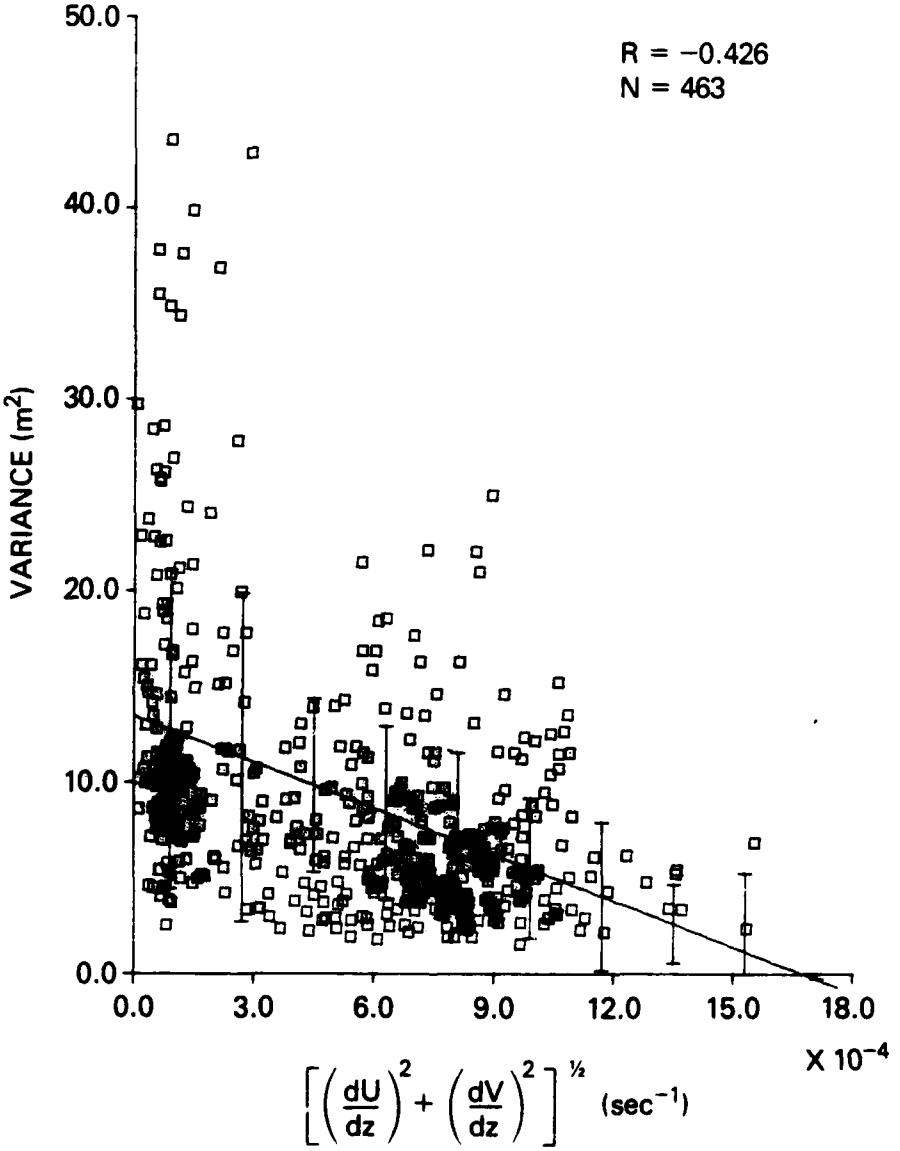

Fig. 5 — Regression of the scaled dropped displacement variance (1 cph) $\langle T'^2 \rangle / (dT/dz)^2$ upon the vertical shear $[(dU/dz)^2 + (dV/dz)^2]^{1/2}$ for both eddy snapshots at depths of 400, 700, 1000, and 1200 m. The correlation coefficient is −0.426 for 463 variance-shear pairs. The error bars represent one standard deviation above and below the fitted line.

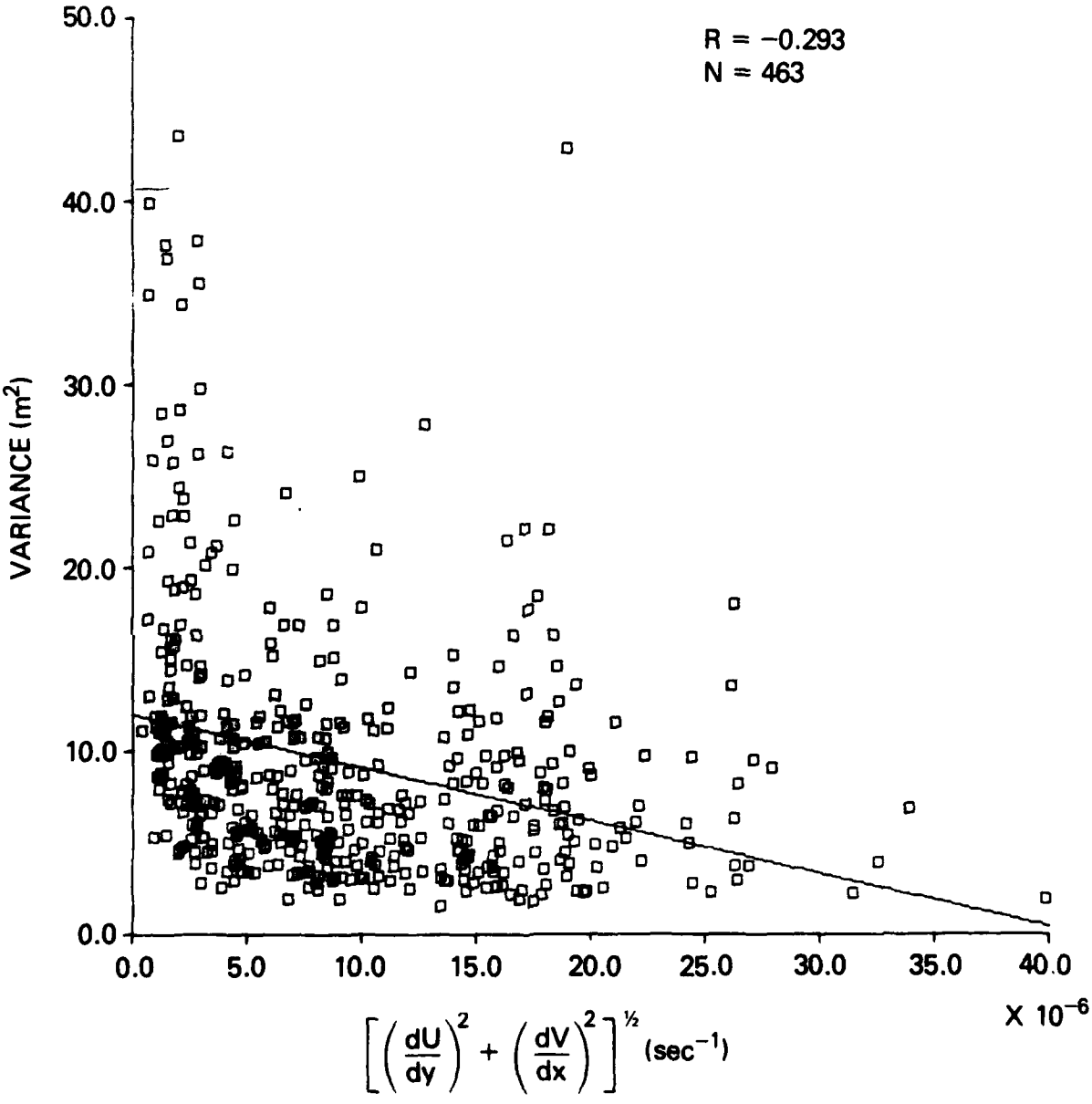

Fig. 6 — Regression of the scaled dropped displacement variance (n/1 cph) $<T'^2>/(dT/dz)^2$ onto the horizontal shear $[(dU/dy)^2 + (dV/dx)^2]^{1/2}$ for both eddy snapshots at depths 400, 700, 1000, and 1200 m. The correlation coefficient is −.293 for 463 variance-shear points.

References

1. Belyayev, V.S. and Yu. V. Nozdrin, 1979: On the vertical spectra of the temperature field fine structure in a frontal zone. Oceanology (USSR) 19, 367-372.

2. Cairns, J.L. and G.O. Williams, 1976: Internal wave observations from a midwater float, 2. J. Geophys. Res. 81, 1943-1949.

3. Desaubies, Y.J.F., 1976: Analytical representation of internal wave spectra. J. Phys. Oceanogr. 6, 976-981.

4. Frankignoul, C., 1976: Observed interaction between oceanic internal waves and mesoscale eddies. Deep Sea Res. 23, 805-820.

5. Gargett, A.E., 1978: Microstructure and fine structure in an upper ocean frontal regime. J. Geophys. Res. 83, 5123-5134.

6. Garrett, C. and W. Munk, 1972: Space-time scales of internal waves. Geophys. Fl. Dyn. 3, 225-264.

7. Garrett, C. and W. Munk, 1975: Space-time scales of internal waves: A progress report. J. Geophys. Res. 80, 291-297.

8. McCartney, M.S., L.V. Worthington, and W.J. Schmitz, Jr., 1978: Large cyclonic rings from the Northeast Sargasso Sea. J. Geophys. Res. 83, 901-914.

9. Mied, R.P. , G.J. Lindemann, and J.M. Bergin, 1983: Azimuthal structure of a cyclonic Gulf Stream ring. J. Geophys. Res. 88, 2530-2596.

10. Mied, R.P. , G.J. Lindemann, and A.F. Schuetz, 1981: The hydrography and dynamics of the FREDDEX eddy. NRL Memorandum Report #4603. Sept. 22.

11. Müller, P. 1976: On the diffusion of momentum and mass by internal gravity waves. J. Fl. Mech. 77, 789-823.

12. Munk, W., 1981: Internal waves and small-scale processes. in Evolution of Physical Oceanography, ed. B.A. Warren and C. Wunsch, MIT Press pp. 264-291.

13. Ruddick, B.R. and T.M. Joyce, 1979: Observations of interaction between the internal wave field and low-frequency flows in the North Atlantic. J. Phys. Oceanogr. 9, 498-517.

14. Williams III, A.J., 1981: The role of double diffusion in a Gulf Stream frontal intrusion. J. Geophys. Res. 86, 1917-1928.

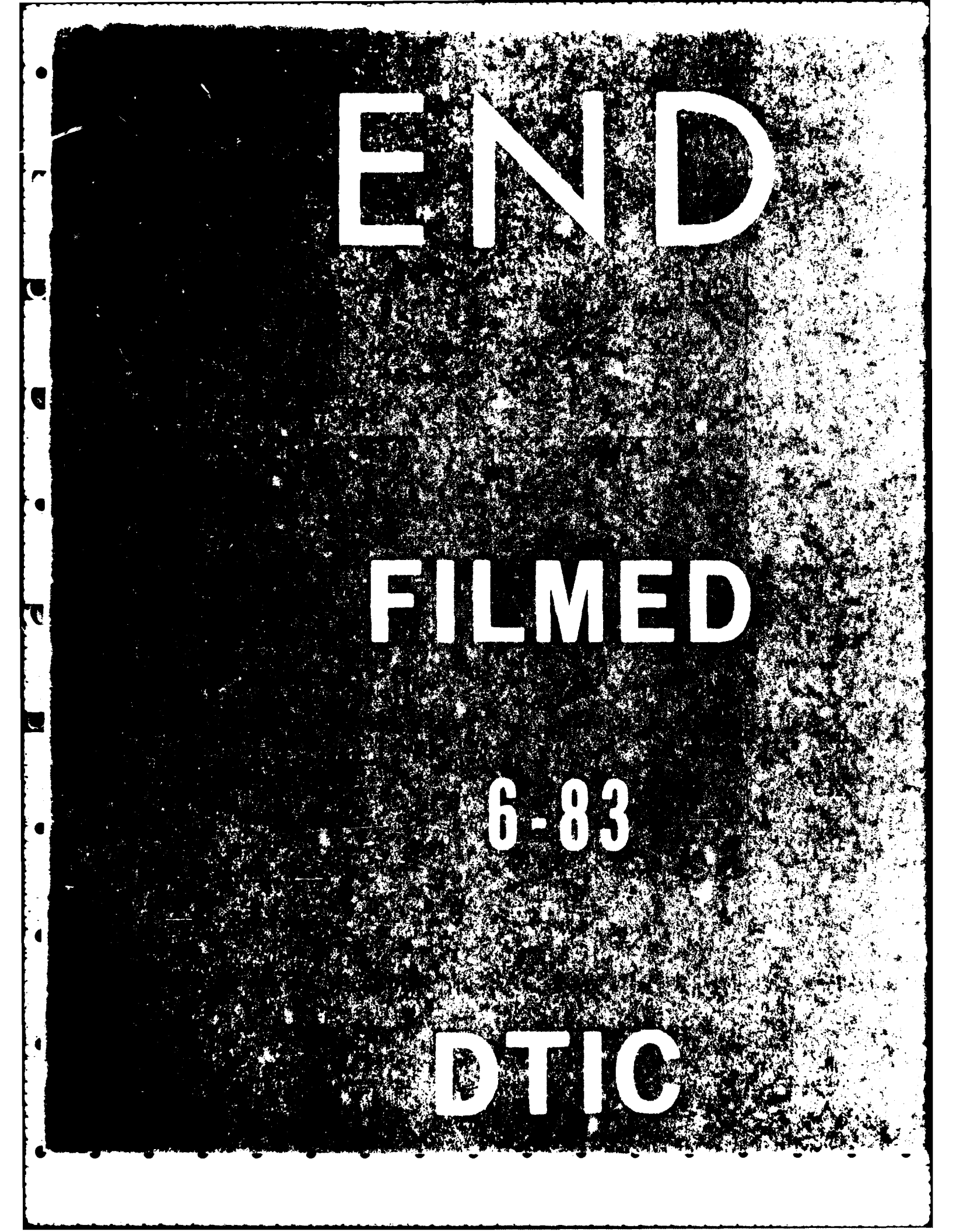
END
FILMED
6-83
DTIC